Dayside Plasma Flows and Ion Heating in the Polar Cap

Leslie Lamarche[1], Roger Varney[1], Ashton Reimer[1]

(1) SRI International, Menlo Park, CA, USA

2022 CEDAR Workshop
Austin, Texas
June 19 – June 24, 2022

Introduction

- Frictional or Joule heating is an important factor in energy deposition in the polar cap ionosphere (Richmond and Thayer, 2013)
- Heating can cause ion outflow, which contributes to magnetosphere-ionosphere coupling dynamics (Howarth and Yau, 2008)
- The Resolute Bay Incoherent Scatter Radar (RISR) is located deep in the polar cap at 82° MLAT and ideally located for observing Joule heating and ion outflow polewards of the cusp (Bahcivan et al., 2010)
- We examine ion heating events observed by RISR in the polar cap and if they can be fully explained by models driven by regional convection and precipitation

Resolute Bay Incoherent Scatter Radar North (RISR-N)

- RISR-N is a ground-based electronically steerable incoherent scatter radar in Resolute Bay, Canada
- Measures plasma density, velocity, and temperatures in 3D volume
- Ideal for imaging large-scale (50–500 km) polar cap dynamics

Ion Heating at RISR

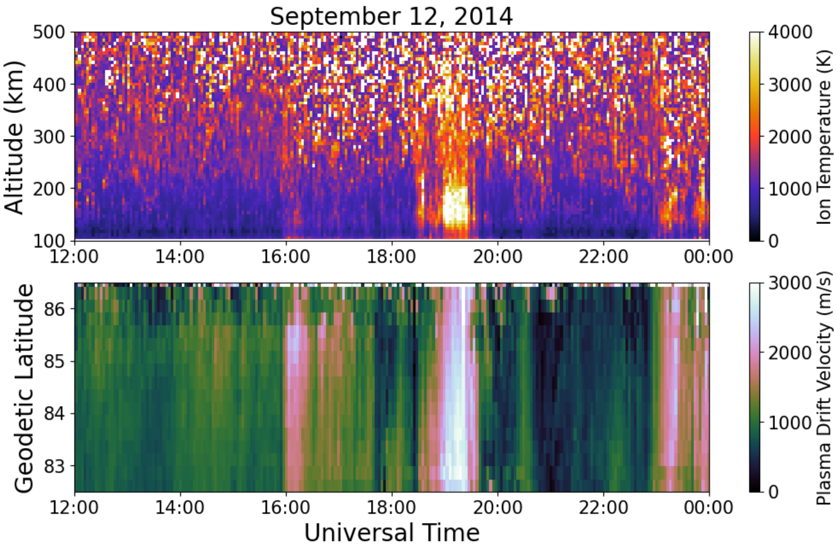

(Clauer et al., 2016)

Convection Climatology in the Polar Cap

Statistical plasma potential patterns from SuperDARN

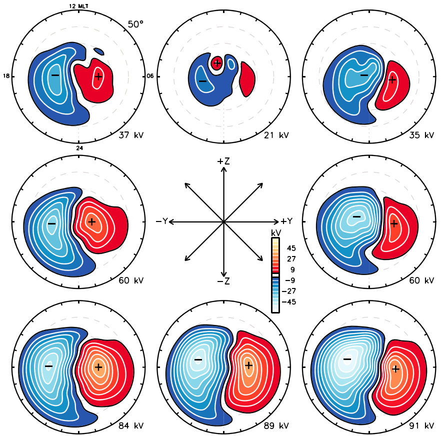

(Thomas and Sheperd, 2018)

Statistical neutral wind patterns from HL-TWiM

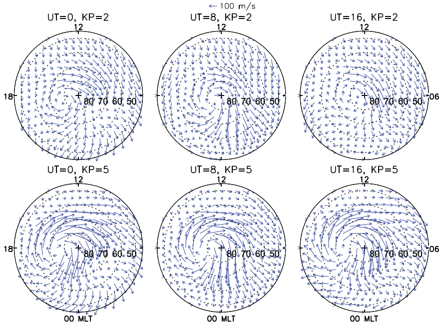

(Dhadly et al., 2019)

Statistical Convection for Northwards IMF

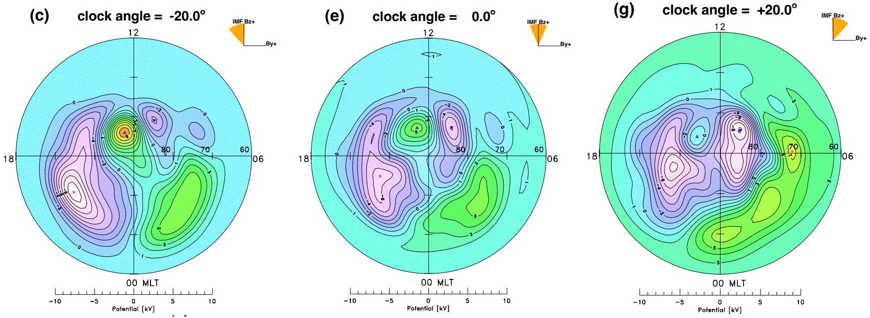

Polar cap convection patterns from Cluster EDI electron drift observations (Förster et al., 2008). Dayside potential patterns are complex, and likely lead to shears and mesoscale flow structuring.

Heating Statistics at RISR

1. Walk the RISR-N database from January 2010 – February 2020 for long-pulse experiments
2. Filter out data points with a large error or "poor fit"
3. Post-integrate all experiments to 5 minute cadence
4. Extract the median plasma parameters (N_e, T_i, T_e) between 300-400 km in the highest elevation beam
5. Use a similar procedure to extract the 3D plasma drift velocity from the RISR-N resolved velocities database (Heinselman and Nicolls, 2008)
6. Compute netural temperature and velocity from empirical models
7. Bin data in MLT and IMF clock angle ($\theta_c = 0$ corresponds to northwards IMF)
8. Average median ion temperature in each bin

Relative Temperature Enhancements

- T_i from RISR-N
- T_n from MSIS-E

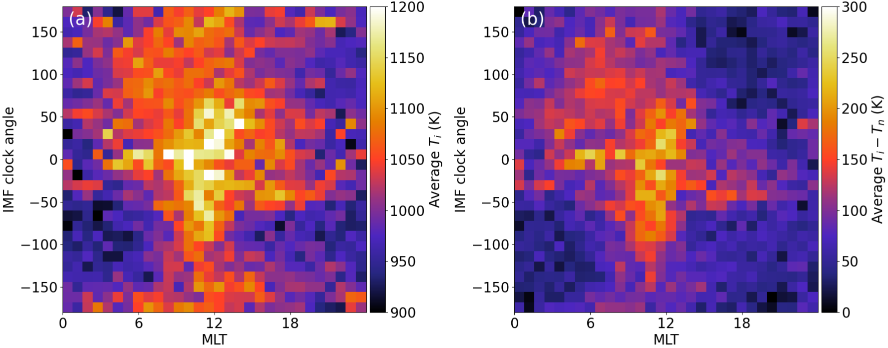

On average, both ion temperatures and relative ion temperature are enhanced in the noon sector under northwards IMF.

Relative Velocity Enhancements

- $\vec{V}_i$ from RISR-N
- $\vec{V}_n$ from HL-TWiM

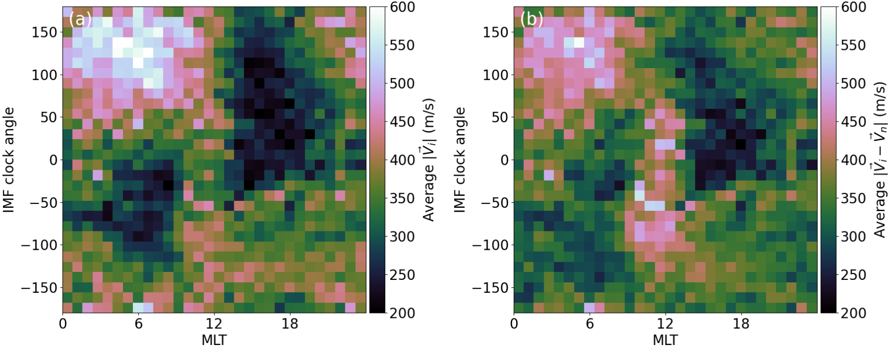

The relative ion velocity is enhanced in the noon sector under northwards IMF, suggesting the ion velocity routinely opposes the statistical neutral velocity.

IPWM

- The Ionosphere/Polar Wind Model (IPWM) is a 3D model of plasma dynamics and ion outflow in the polar cap (Varney et al., 2015)
- Solves eight-moment transport equations for H^+, He^+, and O^+ (^4S) and calculates photochemistry for six other species (Varney et al., 2016)
- Nonorthogonal magnetic dipole coordinate system on approximately 2° grid
- Neutral thermospheric parameters from NRLMSISE-00 (Picone et al., 2002), neutral winds from HL-TWIM (Dhadly et al., 2019), and solar EUV spectrum from HUEVAC (Richards et al., 2006)
- Particle precipitation and plasma convection are driven by empirical or assimilative models to represent realistic conditions

Particle Precipitation - Ovation Prime

- Ovation Prime is a model of discrete and diffuse auroral precipitation, predicting total energy flux, total number flux, and average characteristic energy (Newell et al., 2009, 2010)
- Includes mono-energetic and broadband precipitation, primarily in cusp and auroral region
- Based on decades of DMSP particle energy data

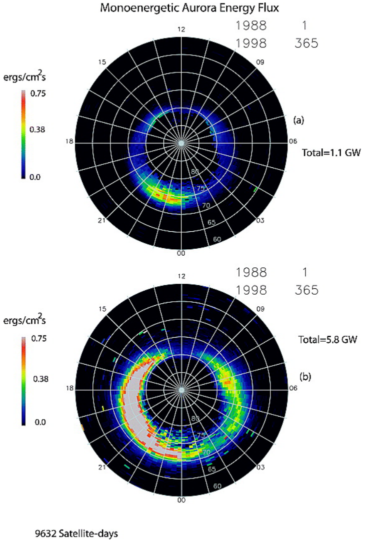

(Newell et al., 2009)

Plasma Convection - SuperDARN

- The Super Dual Auroral Radar Network (SuperDARN) includes a network of high-latitude HF ionospheric radars (Greenwald et al., 1995)
- Line-of-sight velocities measured by individual radars can be inverted to determine the likely convection pattern over the polar cap
- When backscatter is not observed, a statistical pattern is used (Thomas and Sheperd, 2018)

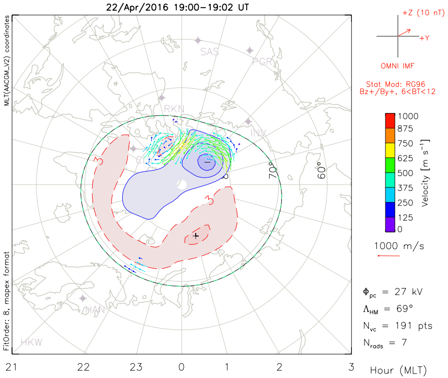

[http://vt.superdarn.org/]

IPWM Results

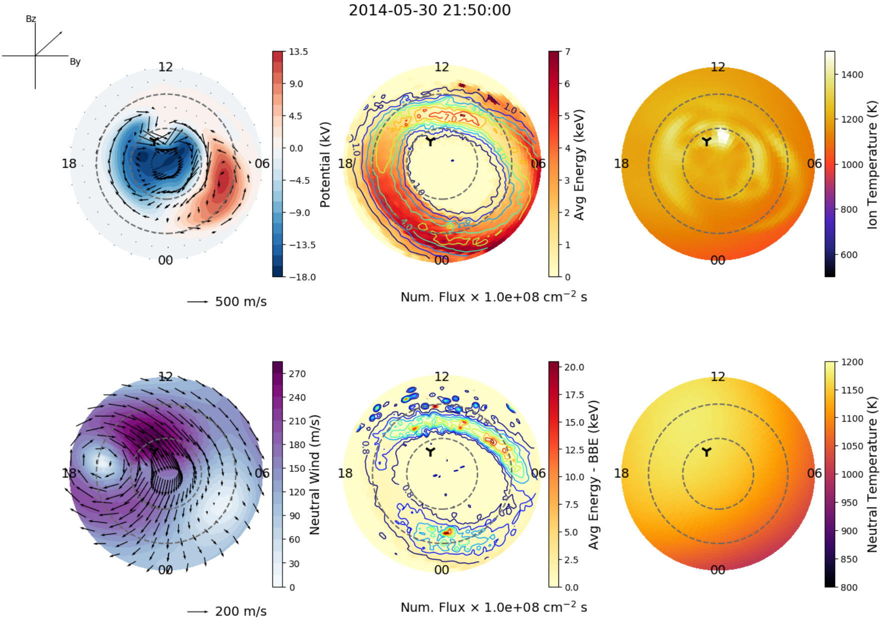

IPWM Comparison with RISR

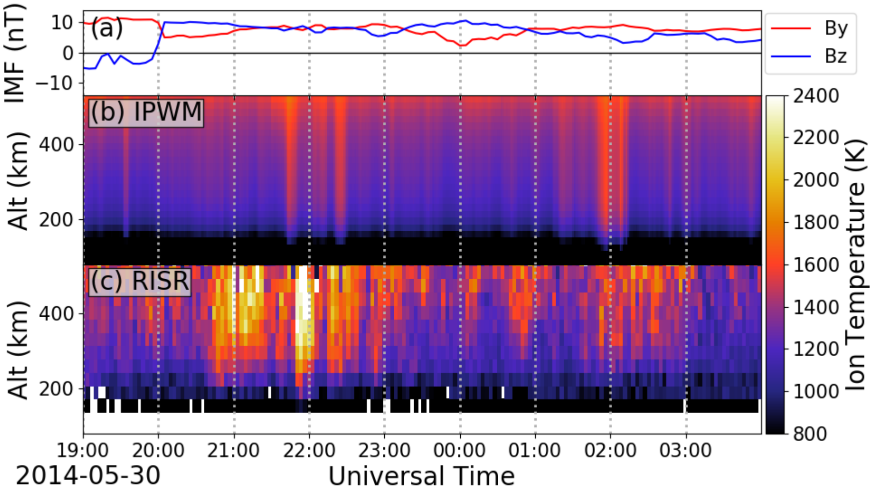

IPWM significantly underestimates the ion temperature during heating events.

Ion Energy Equation

$$\widetilde{T}_i = T_n + \frac{m_n}{3k_B} \left| \vec{V}_i - \vec{V}_n \right|^2 \tag{1}$$

- Reasonable approximation of the ion energy equation in the F-region (St.-Maurice and Hanson, 1982)
- Joule heating rates are equivalent to frictional heating rates under F-region assumptions (Thayer and Semeter, 2004)
- To first order in the F-region, the ion temperature is predominantly determined by the ion-neutral velocity difference

Examine the importance of mesoscale flows by comparing $\widetilde{T}_i$ calculated from the ion energy equation using $\vec{V}_i$ from SuperDARN convection maps (global scale) and RISR (mesoscale) against the measured RISR T_i.

Joule Heating from Ion Energy Equation

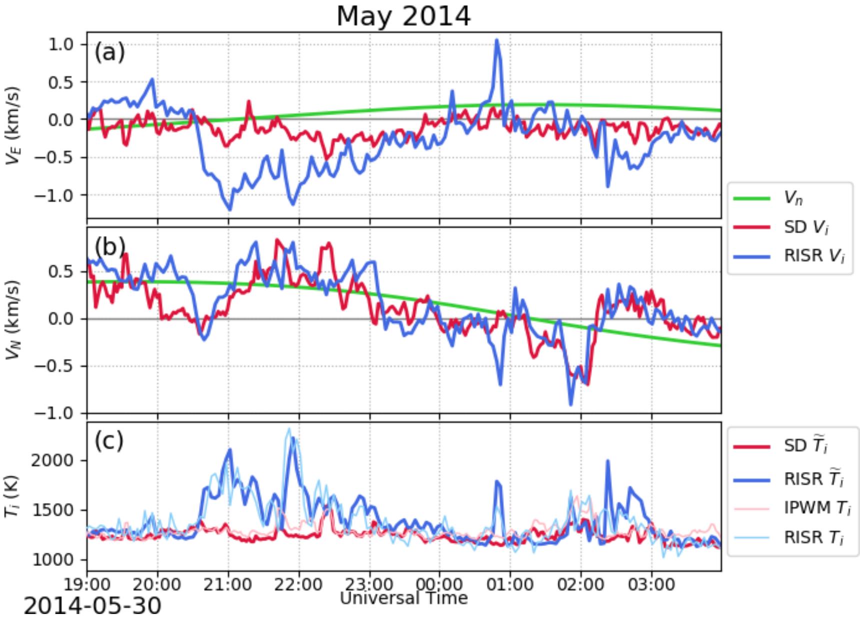

Conclusions

- Ion heating is often observed by RISR, particularly in the noon sector under IMF Bz northwards conditions
- Sunwards flows driven by reconnection in the lobe may be associated with heating events
- Driving IPWM with global-scale convection and precipitation does not produce the extreme heating observed by RISR
- This suggests there are additional factors important for ion heating that are not fully captured by the model and require further investigation
  - Small- and mesoscale flows are not traditionally captured in global-scale convection
  - Neutral winds that oppose the plasma drift velocity can cause enhanced heating
  - Small-scale precipitation features not captured by global models may enhance conductance

Funding Acknowledgments

- NSF Grant AGS-1452191
- NASA Grant 80NSSC21K0458
- Based upon work supported by the Resolute Bay Observatory which is a major facility funded by the National Science Foundation through cooperative agreement AGS-1840962 to SRI International

Lamarche, L. J., Varney, R. H., & Reimer, A. S. (2021). Ion heating in the polar cap under northwards IMF Bz. Journal of Geophysical Research: Space Physics, 126, e2021JA029155.
https://doi.org/10.1029/2021JA029155

References I

Bahcivan, H., Tsunoda, R., Nicolls, M., and Heinselman, C. (2010). Initial ionospheric observations made by the new Resolute incoherent scatter radar and comparison to solar wind IMF. *Geophys. Res. Lett.*, 37.

Clauer, C. R., Xu, Z., Maimaiti, M., Ruohoneimi, J. M., Scales, W., Hartinger, M. D., Nicolls, M. J., Kaeppler, S., Wilder, F. D., and Lopez, R. E. (2016). Investigation of a rare event where the polar ionospheric reverse convection potential does not saturate during a period of extreme northward IMF solar wind driving. *J. Geophys. Res. Space Physics*, 121(6):5422–5435.

Dhadly, M. S., Emmert, J. T., Drob, D. P., Conde, M. G., Aruliah, A., Doornbos, E., Shepherd, G. G., Wu, Q., Makela, J. J., Niciejewski, R. J., Lee, C., Jee, G., and Ridley, A. J. (2019). HL-TWiM empirical model of high-laitude upper thermospheric winds. *J. Geophys. Res. Space Physics*, 124:10592–10618.

Förster, M., Rentz, S., Köhler, W., Liu, H., and Haaland, S. (2008). IMF dependence of high-latitude thermospheric wind pattern derived from CHAMP cross-track measurements. *Ann. Geophysicae*, 26:1581–1595.

Greenwald, R. A., Baker, K. B., Dudeney, J. R., Pinnock, M., Jones, T. B., Thomas, E. C., Villain, J.-P., Cerisier, J.-C., Senior, C., Hanuise, C., Hunsucker, R. D., Sofko, G., Koehler, J., Nielsen, E., Pellinen, R., Walker, A. D. M., Sato, N., and Yamagishi, H. (1995). DARN/SUPERDARN: A global view of the dynamics of high-latitude convection. *Space Sci. Rev.*, 71:761–796.

Heinselman, C. J. and Nicolls, M. J. (2008). A Bayesian approach to electric field and E-region neutral wind estimation with the Poker Flat Advanced Modular Incoherent Scatter Radar. *Radio Sci.*, 43.

Howarth, A. and Yau, A. W. (2008). The effects of IMF and convection on thermal ion outflow inmagnetosphere-ionosphere coupling. *J. Atmos. Sol. Terr. Phys.*, 70:2132–2143.

Newell, P. T., Sotirelis, T., and Wing, S. (2009). Diffuse, monoenergetic, and broadband aurora: The global precipitation budget. *J. Geophys. Res. Space Physics*, 114(A9).

Newell, P. T., Sotirelis, T., and Wing, S. (2010). Seasonal variations in diffuse, monoenergetic, and broadband aurora. *J. Geophys. Res. Space Physics*, 115(A3).

Picone, J. M., Hedin, A. E., Drob, D. P., and Aikin, A. C. (2002). NRLMSISE-00 empirical model of the atmosphere: Statistical comparisons and scientific issues. *J. Geophys. Res.*, 107(A12):1468.

Richards, P. G., Woods, T. N., and Peterson, W. K. (2006). HEUVAC: A new high resolution solar EUV proxy model. *Advances in Space Research*, 37:315–322.

References II

Richmond, A. D. and Thayer, J. P. (2013). *Ionospheric Electrodynamics: A Tutorial*, pages 131–146. American Geophysical Union (AGU).

St.-Maurice, J.-P. and Hanson, W. B. (1982). Ion frictional heating at high latitudes and its possible use for an in situ determination of neutral thermospheric winds and temperatures. *J. Geophys. Res.*, 87(A9):7580–7602.

Thayer, J. P. and Semeter, J. (2004). The convergence of magnetospheric energy flux in the polar atmosphere. *J. Atmos. Sol. Terr. Phys.*, 66:807–824.

Thomas, E. G. and Sheperd, S. G. (2018). Statistical patterns of ionospheric convection derived from mid-latitude, high-latitude, and polar SuperDARN HF radar observations. *J. Geophys. Res. Space Physics*, 123:3196–3216.

Varney, R. H., Wiltberger, M., and Lotko, W. (2015). Modeling the interaction between convection and nonthermal ion outflows. *J. Geophys. Res. Space Physics*, 120:2353–2362.

Varney, R. H., Wiltberger, M., Zhang, B., Lotko, W., and Lyon, J. (2016). Influence of ion outflow in coupled geospace simulations: 1. Physics-based ion outflow model development and sensitivity study. *J. Geophys. Res. Space Physics*, 121:9671–9687.